



Published in final edited form as:

J Comput Assist Tomogr. 2024 ; 48(4): 521–532. doi:10.1097/RCT.0000000000001615.

Diagnostic Anatomic Imaging for Neuroendocrine Neoplasms: Maximizing Strengths and Mitigating Weaknesses

Mina Hesami, MD^{*}, Michael Blake, MD^{*}, Mark A. Anderson, MD^{*}, Luigi Asmundo, MD^{*,†}, Aoife Kilcoyne, MBBCH, BAO^{*}, Zahra Najmi, MD^{*}, Peter D. Caravan, MD^{*}, Ciprian Catana, MD, PhD^{*}, Cynthia Czawlytko, MD^{*}, Shadi Abdar Esfahani, MD^{*}, Avinash R. Kambadakone, MD^{*}, Anthony Samir, MD, PhD^{*}, Shaunagh McDermott, MBBCH, BAO^{*}, Liran Domachevsky, MD[‡], Stephan Ursprung, MD, PhD[§], Onofrio A. Catalano, MD, PhD^{*}

^{*}Department of Radiology, Massachusetts General Hospital, Harvard Medical School, Boston, MA;

[†]Postgraduation School in Radiodiagnosics, Università degli Studi di Milano, Milan, Italy;

[‡]Department of Nuclear Medicine, The Chaim Sheba Medical Center, Tel Hashomer, Israel;

[§]Department of Radiology, University Hospital Tuebingen, Tuebingen, Germany.

Abstract

Neuroendocrine neoplasms are a heterogeneous group of gastrointestinal and lung tumors. Their diverse clinical manifestations, variable locations, and heterogeneity present notable diagnostic challenges. This article delves into the imaging modalities vital for their detection and characterization. Computed tomography is essential for initial assessment and staging. At the same time, magnetic resonance imaging (MRI) is particularly adept for liver, pancreatic, osseous, and rectal imaging, offering superior soft tissue contrast. The article also highlights the limitations of these imaging techniques, such as MRI's inability to effectively evaluate the cortical bone and the questioned cost-effectiveness of computed tomography and MRI for detecting specific gastric lesions. By emphasizing the strengths and weaknesses of these imaging techniques, the review offers insights into optimizing their utilization for improved diagnosis, staging, and therapeutic management of neuroendocrine neoplasms.

Keywords

neuroendocrine neoplasms; carcinoid tumors; CT; MR

Neuroendocrine neoplasms (NENs) represent a complex and diverse group of tumors that have garnered increasing attention within the medical community.¹ Originating from neuroendocrine cells, these tumors can manifest across various anatomical sites, particularly in the gastrointestinal tract and lungs. Their clinical manifestations and heterogeneous histological appearance render their diagnosis and management challenging. As these

neoplasms can vary in size, location, and behavior, the need for accurate and comprehensive imaging techniques is paramount.¹

In the ever-evolving field of medical imaging, multiple techniques have been developed and refined to address the unique challenges posed by NENs. Modalities such as computed tomography (CT) and magnetic resonance imaging (MRI) have become cornerstones in the diagnostic pathway, each offering distinct advantages.² For instance, while CT provides rapid, high-resolution imaging suitable for initial assessments and staging, MRI offers unparalleled soft tissue contrast, making it particularly adept at imaging specific NEN locations. Metabolic imaging, such as positron emission tomography/CT (PET/CT), improves the sensitivity and specificity of NENs detection.²

The importance of understanding the capabilities and constraints of imaging techniques cannot be overstated. Misinterpretation or overreliance on a single modality can lead to diagnostic pitfalls, potentially impacting therapeutic decisions and patient outcomes.³ As such, this article aims to provide a comprehensive review of the imaging modalities pertinent to NENs. By delving into their strengths, weaknesses, and tailored protocols, we aim to equip healthcare professionals with the knowledge necessary to optimize their use.^{4,5}

In the subsequent sections, readers will be introduced to the nuances of imaging techniques, their applications in specific clinical scenarios, and the potential challenges and pitfalls to be wary of. The goal is to foster a deeper understanding of the role of imaging in the context of NENs, promoting informed decision making and advancing patient care.

IMAGING

Although histopathological confirmation represents the gold standard for diagnosing NENs, imaging is critically important in diagnosing, staging, assessing response to therapy, and localization of the organ of origin in the case of tumors of unknown primary.² Morphologic imaging, such as CT, MRI, and endoscopic ultrasound (EUS), are used for tumor detection, diagnosis, staging, and restaging. Some CT and MR techniques, for example, perfusion and diffusion-weighted imaging (DWI), can also evaluate functional features, including cellular density and blood flow. Because of the large variability of the organ of origin, stage at presentation, and biological heterogeneity of NENs, a single radiological modality is unlikely to be completely effective in detecting and characterizing all these tumors. Metabolic imaging such as PET/CT improves the sensitivity and specificity of NEN detection to 80%–90%⁵ and is described in a separate article in this journal. The small size and variable locations of NENs hamper the detection of primary tumors by CT and MRI.⁶ However, these techniques are typically used for the initial diagnostic workup of NENs and restaging. CT and MRI performances are strongly influenced by the acquisition protocols, which should be tailored according to the specific clinical questions, for example, suspected small bowel NEN (SB-NEN) versus suspected primary gastric NEN (gNEN) or pancreatic NEN (pNEN).

Both CT and MRI utilize the concept of multiphase or dynamic contrast imaging. However, MRI has a higher sensitivity than CT.⁷ MRI is typically superior to CT in imaging the

liver and pancreas due to the improved soft tissue contrast.⁸ Another benefit of MRI is that ionizing radiation is not utilized. However, MRI is often less accessible and more expensive than CT. As a result, it is not commonly used as a standard imaging method for all NENs but is instead employed for specific types of NENs, including pNENs and rectal NENs (rNENs). It is also used as a problem-solving method when CT is inadequate.

EUS, combining high-resolution morphologic information with the ability to obtain tissue samples, is the preferred imaging technique for diagnosing pNENs and for locally assessing gNENs, duodenal NENs (dNENs), rNENs, and pNENs.^{9,10} However, EUS highly relies on the operator's expertise, making it a technically demanding procedure, besides being invasive and costly. All the protocols are summarized in Table 1.

Pancreatic Neuroendocrine Neoplasms

Clinically, pNENs can be categorized as functioning or nonfunctioning, depending on their association with a specific clinical syndrome caused by hormone overproduction.¹¹ Nonfunctioning pNENs may be asymptomatic in the early stages, allowing for greater tumor growth and larger tumors at diagnosis.¹² On the other hand, functioning pNENs are usually smaller at diagnosis, in the range of 1–2 cm in diameter.¹³ Nonfunctioning pNENs, comprising 60%–80% of cases, often present as large pancreatic masses with a heterogeneous enhancement pattern due to necrosis and hemorrhage.^{14,15} CT is the preferred initial imaging modality for evaluating patients suspected of having.

pNENs with a protocol includes upper abdomen precontrast, arterial, and pancreatic phase images as well as chest, abdomen, and pelvis venous phase scans.¹⁶ The CT detection rate of pNENs ranges from 69% to 94%, and the sensitivity varies from 63% to 96%.^{14,17–19} Because of the hypervascular nature of pNENs, the arterial phase is more advantageous and shows higher sensitivity (83%–88%) compared to the venous phase (11%–76%), particularly for small tumors such as insulinomas.^{13,20} Insulinomas exhibit homogeneously increased density in both the arterial and pancreatic phases, while gastrinomas typically have less vascularity and may show more intense delayed enhancement due to fibrosis.¹⁴ The presence of ductal involvement in pNENs is associated with higher-grade tumors²¹; CT demonstrated a sensitivity of 88.8% and specificity of 92.8% in detecting main pancreatic duct involvement, whereas MRI exhibited a sensitivity of 100% and specificity of 95.2%.²² However, CT might be superior to MRI in evaluating the extent of vascular invasion.²²

Dual-energy CT (DECT) has the potential to enhance the visibility of pNENs by highlighting subtle differences in attenuation between the tumors and the surrounding background. DECT enables the preoperative detection of insulinomas with a high sensitivity compared with conventional CT (95.7% vs 68.8%).²³ DECT with monoenergetic low keV (55 keV) images improves the detection of pNENs.²⁴

The MRI protocol for NENs usually consists of T1-weighted (T1W) dual gradient echo (GE), T2-weighted (T2W) fast spin echo, dynamic three-dimensional (3D) T1W GE acquired before and after injecting a gadolinium chelate that encompasses arterial, venous, and delayed (>5 minutes) phases, as well as DWI sequences and magnetic resonance cholangiopancreatography (MRCP) images.²¹ The application of fat suppression on T1W

and T2W images is beneficial for enhancing the intrinsic contrast between the pancreatic tumor and the surrounding normal pancreatic tissue²¹; pNENs typically show low signal intensity on T1W images and mildly high signal intensity on T2W images. Arterial phase images are the most effective for detecting the hypervascularity of pNENs (Fig. 1).²⁵ For nonhypervascular tumors, DWI and T1W fat-saturated images provide the highest detection yield.²⁶ Precontrast T1W fat-saturated sequences can also be helpful in overcoming the imaging pitfall of some tumors that might be isointense with the background parenchyma after contrast injection, rendering them undetectable on the postcontrast images. MRI has a 75%–95% sensitivity in detecting pNENs, with lower performance rates in cases degraded by respiratory motion.^{8,27–30} Tumor size also impacts its sensitivity, being 60%–95% for lesions >2.5 cm versus 34% for lesions <1.5 cm.³¹

EUS is especially well-suited for detecting small pancreatic lesions, such as insulinomas and gastrinomas, with detection rates ranging from 79% to 94%.^{32,33} Although EUS is typically used alongside other imaging modalities, in addition to confirming the size and morphologic features of pNENs, it can also allow tissue sampling (Fig. 2).³⁴ EUS showed a higher sensitivity than CT (91.7% vs 63.3%), particularly for insulinomas (84.2% vs 31.6%) and successfully detected 20 out of 22 CT-negative tumors in a study.³⁵ Another advantage of EUS is its ability to evaluate peripancreatic abnormalities, such as lymph nodes and vessels.²⁵ However, EUS may overestimate the size of pNENs > 2 cm, while MRI provides more accurate measurements.³⁶ EUS heavily relies on the expertise and skill of the endosonographer and is an invasive procedure.³⁷

Cystic pNENs are a rare subtype, usually nonfunctioning, with a better prognosis than solid pNENs.³⁸ The increased utilization of cross-sectional imaging has led to a rise in the detection of cystic pNENs.³⁹ Typically, cystic changes are seen in large lesions. However, significant cystic transformation can occur in small pNENs as well.¹⁵ Cystic pNENs are hard to differentiate from other cystic lesions such as mucinous cystic neoplasms, serous cystadenomas, side branch intraductal papillary mucinous neoplasm, or necrotic tumors on cross-sectional imaging.^{40,41} An enhancing rim is highly suggestive of cystic pNENs (Fig. 3) and was seen in 85% of cystic pNENs and is best appreciated in arterial phase imaging.⁴¹ MRI outperforms CT in detecting tumor hypervascularity, especially peripheral rim enhancement.²² The following features help in the differential diagnosis of cystic pancreatic lesions.

Intraductal papillary mucinous neoplasm typically lacks wall enhancement and shows pancreatic duct communication (Fig. 4).⁴² Multiple thin enhancing internal septa, microcystic internal structure with lobulations, and central calcification help distinguish serous cystadenomas.⁴³ Mucinous cystic neoplasms (Fig. 5) are difficult to differentiate from conventional imaging but may have a slightly lobulated contour, contain internal septa, and lack DOTA uptake in PET—a feature that is observed even in cystic pNENs (Fig. 6).

Gastroduodenal Neuroendocrine Neoplasms

The initial identification of gNENs is typically done through EUS, which plays a crucial role in their evaluation.⁴⁴ EUS is frequently conducted to assess the depth of invasion, presence of adjacent lymph node metastases and to help plan the treatment strategy in

gNENs >1 cm.⁴⁵ This technique has a sensitivity of 94% in detecting candidates suitable for endoscopic resection.⁴⁶ Type 1 and 2 gNENs present as small single or multiple markedly arterially enhancing, well-defined, polypoid lesions/type 3 gNENs appear as a single, large, and variably enhancing mass, indistinguishable from other more common types of gastric malignancies.⁴⁷

Duodenal gastrinomas comprise 50%–60% of all dNENs, mostly occur within the gastrinoma triangle (70%–85% of cases), and are characteristically small with 77% of them being <1 cm.⁴⁸ The gastrinoma triangle is bounded superiorly by the confluence of the cystic and common bile ducts, inferiorly by the junction of the second and third portions of the duodenum, and medially by the junction of the neck and body of the pancreas. The majority of duodenal gastrinomas are solitary, but 10%–25% of cases occur in patients with MEN-1, often presenting as multiple tumors and some of them can be as small as <5 mm.⁴⁹ CT scans with thin slices in both arterial and venous phases, along with multiplanar coronal and sagittal reconstructions can effectively detect these lesions.⁴⁹ Although the ability of EUS to detect small duodenal tumors is controversial, it demonstrated higher sensitivity in detection of duodenal gastrinomas compared with CT and MRI (79%, 69%, and 61%, respectively).⁵⁰ Most dNENs are found in the first and second portion of the duodenum and are small at the time of diagnosis. Therefore, their detection is challenging for anatomical imaging techniques as well as for EUS (sensitivity <50%).^{7,51} They mostly appear as well-defined, hypoechoic, rounded masses with a “salt and pepper” appearance at EUS.⁵² Ampullary NENs are rare, but given the potential to cause biliary and pancreatic duct obstruction, they can rise to clinical attention very early and be diagnosed even when extremely small (Fig. 7).⁵³

EUS is crucial in identifying loco-regional lymph node metastases⁵⁴ and is commonly used for diagnosing gastroduodenal NENs. The role of CT, once the primary site is established, is to identify regional and distant metastases, aiding in disease staging.¹³ CT protocol is based on upper abdominal arterial phase imaging and chest, abdomen, and pelvis portal venous phase scans. Water or other neutral oral contrast should be administered shortly before scanning to ensure optimal distension of the stomach and duodenum.⁴⁴

Although the cost-effectiveness of CT and MRI is questionable when detecting small type 1 and 2 gastric lesions, their significance for disease staging is highlighted in advanced neoplasms and type 3 gNENs.⁵⁵ On the other hand, dNENs pose significant diagnostic challenges, given their small size at clinical presentation.

Small Bowel Neuroendocrine Neoplasms

The distal ileum is the most common site of SB-NENs, which tend to occur in the distal 100 cm of the ileum.⁵⁶ Generally, jejunoileal NENs are thought to have more malignant potential, with regional or distant metastases often observed even with small lesions.⁵⁷ Primary tumors in the small bowel can lead to complications such as bowel obstruction or fibrosis. Diagnosing SB-NENs is difficult using morphologic imaging studies. Mesenteric lymph node metastases with accentuated desmoplastic reaction are the most common imaging findings in such patients (Fig. 8).⁵⁸ However, larger lesions may be visualized on CT, especially if they result in complications such as obstruction.⁵⁹ To optimize

the visualization of these lesions, a contrast-enhanced CT enterography protocol with negative oral contrast and spasmolytic agents is recommended (Fig. 9).⁶⁰ CT enterography demonstrated a sensitivity and specificity of 85% and 97% in detecting primary NENs in the small bowel.^{60,61} MRI is less commonly used but SB-NENs typically appear hypointense on T1W, hyperintense on T2W images, with enhancement and diffusion restriction.⁶² An entero-MRI protocol that includes negative oral and intravenous contrast agents in these settings may facilitate primary NEN detection (Fig. 10).

Colorectal Neuroendocrine Neoplasms

NENs of the rectum are typically small and localized at the time of diagnosis; on the other hand, colonic NENs are aggressive, poorly differentiated, large, and typically metastatic at initial presentation.⁵⁶ CT can be of limited value for assessing rNENs given their small size, but EUS can accurately detect and delineate the tumor from the surrounding tissues and assess the depth of invasion.⁶³ The reported sensitivity of EUS for evaluation of tumor depth ranges from 76% to 93%.⁶⁴ As a result, EUS has become a crucial examination for precise localization and delineation of rNENs, tissue sampling, and local staging.⁵⁶ MRI of rNENs is useful for assessing local spread and determining surgical resectability.⁶⁵ MRI acquisition protocols for rNENs are analogous to high-resolution rectal cancer MRI acquisition protocols. CT and MRI stage colorectal NENs by detecting regional and distant metastases and evaluating infiltration into adjacent organs in locally advanced tumors.^{13,66}

Lung

Lung NENs (LuNENs) are categorized as central (70% of tumors) or peripheral, based on their origin relative to the bronchial tree.⁶⁷ Diffuse idiopathic pulmonary neuroendocrine cell hyperplasia (DIPNECH) can be recognized as a precursor for LuNENs, particularly peripheral LuNENs.⁶⁸ DIPNECH has nonspecific clinical presentation such as cough and asthma-like symptoms; therefore, it might be initially misdiagnosed. CT findings in DIPNECH are represented by multiple pulmonary nodules, small airways obstruction with bronchial wall thickening, inspiratory mosaic attenuation, and expiratory air trapping (Fig. 11).⁶⁸ Mosaic attenuation has been the predominant observation in DIPNECH on CT and is highly suggestive of DIPNECH in conjunction with multiple small nodules.⁶⁹ When mosaic attenuation is not visible on CT, it is crucial to perform additional expiration CT scans to detect air trapping, which serves as an indirect sign of small airway obstruction in DIPNECH.⁶⁹ Small pulmonary nodules are also frequently observed, and given the close association between DIPNECH and LuNENs, any nodule ≥ 5 mm in the setting of DIPNECH should raise suspicion for the presence of LuNENs.⁷⁰ NENs arising from DIPNECH exhibit similar behavior to those without DIPNECH.⁷¹

LuNENs are separated into the following four categories: typical carcinoid tumor (TC), atypical carcinoid tumor (AC), large-cell neuroendocrine carcinoma (LCNEC), and small-cell lung carcinoma (SCLC).⁷²

Carcinoids are slow-growing and well-differentiated tumors, whereas LCNEC and SCLC are highly aggressive and poorly differentiated tumors (Figs. 12–13).⁷³ Most TCs are centrally located, whereas ACs tend to be larger in size and are frequently found peripherally,

however they share similar imaging characteristics.⁷⁴ LCNECs tend to present as large peripheral masses, whereas SCLCs are large central or mediastinal masses with involvement of the hilum in up to 85% of cases.⁷⁴ CT is the preferred imaging modality for assessing lung lesions and is the recommended diagnostic tool for centrally located LuNENs; thus, it should be the first-line imaging in patients with LuNENs.⁶⁷ Peripheral LuNENs appear as round or ovoid solitary nodules with smooth or lobulated borders and high attenuation on contrast-enhanced CT.⁷⁵ Both TC and AC can be associated with hilar or mediastinal lymphadenopathy, which is well appreciated on CT.⁷⁴ Moreover, LuNENs tend to be vascular and may show significant enhancement.⁷⁶ They usually show a nonspecific low or intermediate-signal intensity on T1W images and high-signal intensity on T2W images.⁷⁷ Although the utilization of MRI for identifying LuNENs is limited, mediastinal MRI can be advantageous in cases of inconclusive CT.⁷⁸

Neuroendocrine Neoplasms of Unknown Primary

In about 13% of NEN patients, the primary site is initially unknown⁷⁹ and the algorithm for their workup depends on the clinical scenario. However, in most of such cases, the organ of origin is the intestine or the lungs.⁷⁹ CT is the most commonly used modality for identifying an unknown primary tumor site.⁸⁰

Although the location of tumor affects the detection capability of CT, its mean sensitivity is 73%.^{14,18,19}

Investigation of the small bowel is essential as it is the most common primary site of NENs; nuclear medicine methods and CT enterography can be employed in these settings.⁸¹ When conventional imaging methods fail to identify the primary site of NENs, DOTA PET/CT can be successfully used and has shown a sensitivity of 60.78% in revealing the elusive primary site.⁸¹ Neoplasms with unknown primaries carry a poorer prognosis, so identifying the primary site is important to appropriately tailor management of such patients.⁸²

Metastases

The most common sites of metastases in NENs are the liver (19.7%), distant lymph nodes (16.9%), lungs (15.7%), bones (12.6%), central nervous system (8.6%), and peritoneum (8.2%).⁸³ SB-NENs are the most common to metastasize, with the liver being the primary target.⁸² On the other hand, appendiceal NENs, rNENs, and gNENs have lower metastatic potential.⁵⁶ MRI is the best conventional study to detect liver metastases in NENs.⁸⁴ MRI acquisition of the liver commonly includes fat-suppressed T2W, DWI, and dynamic contrast-enhanced T1W images.⁸⁵ Liver metastases are usually hypervascular but may show different patterns of gadolinium enhancement; hence, it is essential to perform multiphase contrast-enhanced MRI.⁸⁶ The sensitivity of DWI (71.6%) is higher than T2W (55.6%) and dynamic contrast-enhanced T1W (47.5%–48.1%) in identifying liver metastases from NENs.⁸⁷ Utilizing hepatobiliary contrast agents improve NEN metastases detection and facilitates reproducibility of measurement of metastatic liver lesions on follow-up imaging.⁸⁸ CT, on the other hand, showed mean sensitivity of 75% and 82% in the detection of extrahepatic and hepatic metastases, respectively. Preliminary data point out improved performances with DECT (Fig. 14).^{14,18,19}

Patterns of lymph node involvement are influenced by the location of the primary lesion. Regional lymph nodes are the most frequent metastatic sites in pancreatic and SB-NENs.^{89,90} Moreover, lymph node metastases have been reported in 11%–50% of dNENs.⁴⁷ EUS can efficiently assess the regional lymph nodes in rNENs with a sensitivity of 61%–88%.^{64,91} Additionally, EUS is an excellent modality for visualization and sampling of upper abdominal lymph nodes.⁹² CT has a relatively low sensitivity of 27% for detecting lymph node metastases.⁹³ Whole-body MRI has a 73% sensitivity for lymph node detection compared with 100% of PET/CT.⁹⁴

Bone metastases occur in up to one-third of patients with liver metastases and should be sought in all patients.⁹⁴ Bone metastases in NENs are associated with poor prognosis and appear predominantly osteoblastic (up to 83%).^{95,96} MRI is the most sensitive (95%) modality for the evaluation of osseous metastatic diseases with a sensitivity up to 100%.^{95,97} Bone lesions are hyperintense on T2W and short tau inversion recovery (STIR) sequences, demonstrating avid enhancement.⁷⁴ One limitation of MRI is that it cannot effectively evaluate the cortical bone, given its short T2 relaxation time. Consequently, bones with low marrow volume, such as the ribs, are more effectively assessed by CT.⁹⁸ CT provides exceptional resolution to visualize cortical and trabecular bone which aids in the detection of osteolytic and osteosclerotic metastases.⁹⁸ However, radiographic characteristics of early osseous metastases are usually subtle, and these lesions may be easily missed on CT (Fig. 15). Notably, bone metastases may remain abnormal on CT after treatment.⁹⁵ CT showed a sensitivity of 58% compared with 92% of PET for detecting bone metastases in NENs.⁹⁵ Therefore, guidelines recommend the use of SSSTR PET for the detection of metastatic osseous lesions in NENs.⁹⁹

The lung is also a common site for metastases in NENs, and a dedicated chest CT is the best imaging modality for their evaluation.⁹² CT can assess the extent of metastases and determine the involvement of mediastinal lymph nodes.¹⁰⁰ MRI can be a useful tool for evaluating the neural foramen or brachial plexus involvement in case of any suspicious clinical or CT findings.¹⁰⁰

CONCLUSION

In diagnosing and characterizing NENs, imaging techniques are indispensable tools. Despite the inherent challenges posed by NENs' diverse manifestations and locations, modalities like CT and MRI have showcased their efficacy. CT is instrumental for initial assessments and comprehensive staging, whereas MRI excels in delineating details of liver, pancreatic, and osseous structures. However, it is paramount to acknowledge the limitations of these tools, from MRI's constraints in assessing cortical bone to the debated cost-effectiveness in detecting certain lesions. Embracing the strengths and weaknesses of these imaging techniques will pave the way for tailored protocols, optimizing diagnosis, staging, and therapeutic strategies for NENs. As the medical field continues to evolve, it remains crucial to refine these modalities for more precise and effective patient care.

Funding statement:

This research did not receive any specific grant from funding agencies in the public, commercial, or not-for-profit sectors.

REFERENCES

1. Haider M, Al-Toubah T, El-Haddad G, et al. Molecular imaging and radionuclide therapy of neuroendocrine tumors. *Curr Opin Endocrinol Diabetes Obes.* 2020;27:16–21. [PubMed: 31789833]
2. Rizen EN, Phan AT. Neuroendocrine tumors: a relevant clinical update. *Curr Oncol Rep.* 2022;24:703–714. [PubMed: 35254612]
3. Rindi G, Mete O, Uccella S, et al. Overview of the 2022 WHO classification of neuroendocrine neoplasms. *Endocr Pathol.* 2022;33: 115–154. [PubMed: 35294740]
4. Neuroendocrine tumors - statistics. Cancer.net Available at: <https://www.cancer.net/cancer-types/neuroendocrine-tumors/statistics> (2012). Accessed January 3, 2023.
5. Bodei L, Sundin A, Kidd M, et al. The status of neuroendocrine tumor imaging: from darkness to light? *Neuroendocrinology.* 2015;101:1–17. [PubMed: 25228173]
6. Treglia G, Castaldi P, Rindi G, et al. Diagnostic performance of gallium-68 somatostatin receptor PET and PET/CT in patients with thoracic and gastroenteropancreatic neuroendocrine tumours: a meta-analysis. *Endocrine.* 2012;42:80–87. [PubMed: 22350660]
7. Morse B, Al-Toubah T, Montilla-Soler J. Anatomic and functional imaging of neuroendocrine tumors. *Curr Treat Options in Oncol.* 2020; 21:75.
8. van Essen M, Sundin A, Krenning EP, et al. Neuroendocrine tumours: the role of imaging for diagnosis and therapy. *Nat Rev Endocrinol.* 2014;10: 102–114. [PubMed: 24322649]
9. Koffas A, Giakoustidis A, Papaefthymiou A, et al. Diagnostic work-up and advancement in the diagnosis of gastroenteropancreatic neuroendocrine neoplasms. *Front Surg.* 2023;10:1064145. [PubMed: 36950054]
10. Zilli A, Arcidiacono PG, Conte D, et al. Clinical impact of endoscopic ultrasonography on the management of neuroendocrine tumors: lights and shadows. *Dig Liver Dis.* 2018;50:6–14. [PubMed: 29102525]
11. Klöppel G Classification and pathology of gastroenteropancreatic neuroendocrine neoplasms. *Endocr Relat Cancer.* 2011; 18(Suppl 1):S1–S16. [PubMed: 22005112]
12. Wang S-E, Su CH, Kuo YJ, et al. Comparison of functional and nonfunctional neuroendocrine tumors in the pancreas and peripancreatic region. *Pancreas.* 2011;40:253–259. [PubMed: 20966805]
13. Sundin A, Arnold R, Baudin E, et al. ENETS consensus guidelines for the standards of care in neuroendocrine tumors: radiological, nuclear medicine & hybrid imaging. *Neuroendocrinology.* 2017;105:212–244. [PubMed: 28355596]
14. Hofland J, Refardt JC, Feelders RA, et al. Approach to the patient: insulinoma. *J Clin Endocrinol Metab.* 2023;109:dgad641.
15. Tamm EP, Bhosale P, Lee JH, et al. State-of-the-art imaging of pancreatic neuroendocrine tumors. *Surg Oncol Clin N Am.* 2016;25:375–400. [PubMed: 27013371]
16. Gregucci F, Fiorentino A, Mazzola R, et al. Radiomic analysis to predict local response in locally advanced pancreatic cancer treated with stereotactic body radiation therapy. *Radiol Med.* 2022;127:100–107. [PubMed: 34724139]
17. Gouya H, Vignaux O, Augui J, et al. CT, endoscopic sonography, and a combined protocol for preoperative evaluation of pancreatic insulinomas. *AJR Am J Roentgenol.* 2003;181:987–992. [PubMed: 14500214]
18. Sundin A, Vullierme MP, Kaltsas G, et al. ENETS consensus guidelines for the standards of care in neuroendocrine tumors: radiological examinations. *Neuroendocrinology.* 2009;90:167–183. [PubMed: 19077417]
19. Javed AA, Zhu Z, Kinny-Köster B, et al. Accurate non-invasive grading of nonfunctional pancreatic neuroendocrine tumors with a CT derived radiomics signature. *Diagn Interv Imaging.* 2024;105:33–39. [PubMed: 37598013]

20. Kim JH, Eun HW, Kim YJ, et al. Pancreatic neuroendocrine tumour (PNET): staging accuracy of MDCT and its diagnostic performance for the differentiation of PNET with uncommon CT findings from pancreatic adenocarcinoma. *Eur Radiol.* 2016;26:1338–1347. [PubMed: 26253257]
21. Dromain C, Déandréis D, Scoazec JY, et al. Imaging of neuroendocrine tumors of the pancreas. *Diagn Interv Imaging.* 2016;97:1241–1257. [PubMed: 27876341]
22. Foti G, Boninsegna L, Falconi M, et al. Preoperative assessment of nonfunctioning pancreatic endocrine tumours: role of MDCT and MRI. *Radiol Med.* 2013;118:1082–1101. [PubMed: 23801403]
23. Lin XZ, Wu ZY, Tao R, et al. Dual energy spectral CT imaging of insulinoma—value in preoperative diagnosis compared with conventional multi-detector CT. *Eur J Radiol.* 2012;81:2487–2494. [PubMed: 22153746]
24. Hardie AD, Picard MM, Camp ER, et al. Application of an advanced image-based virtual monoenergetic reconstruction of dual source dual-energy CT data at low keV increases image quality for routine pancreas imaging. *J Comput Assist Tomogr.* 2015;39:716–720. [PubMed: 26196343]
25. Lee DW, Kim MK, Kim HG. Diagnosis of pancreatic neuroendocrine tumors. *Clin Endosc.* 2017;50:537–545. [PubMed: 29207856]
26. Anaye A, Mathieu A, Closset J, et al. Successful preoperative localization of a small pancreatic insulinoma by diffusion-weighted MRI. *JOP.* 2009; 10:528–531. [PubMed: 19734630]
27. Yang Y, Shi J, Zhu J. Diagnostic performance of noninvasive imaging modalities for localization of insulinoma: a meta-analysis. *Eur J Radiol.* 2021;145:110016. [PubMed: 34763145]
28. Caramella C, Dromain C, De Baere T, et al. Endocrine pancreatic tumours: which are the most useful MRI sequences? *Eur Radiol.* 2010;20: 2618–2627. [PubMed: 20668861]
29. Antwi K, Wiesner P, Merkle EM, et al. Investigating difficult to detect pancreatic lesions: characterization of benign pancreatic islet cell tumors using multiparametric pancreatic 3-T MRI. *PLoS One.* 2021; 16:e0253078. [PubMed: 34115803]
30. Berbís MÁ, Godino FP, Rodríguez-Comas J, et al. Radiomics in CT and MR imaging of the liver and pancreas: tools with potential for clinical application. *Abdom Radiol (NY).* 2023;49:322–340. [PubMed: 37889265]
31. Lee L, Ito T, Jensen RT. Imaging of pancreatic neuroendocrine tumors: recent advances, current status, and controversies. *Expert Rev Anticancer Ther.* 2018;18:837–860. [PubMed: 29973077]
32. Chandra A, Hati A. Endoscopic ultrasound: a very important tool in detecting small insulinomas. *QJM.* 2022;115:308–309. [PubMed: 35266542]
33. Manta R, Nardi E, Pagano N, et al. Pre-operative diagnosis of pancreatic neuroendocrine tumors with endoscopic ultrasonography and computed tomography in a large series. *J Gastrointest Liver Dis.* 2016;25: 317–321. [PubMed: 27689195]
34. Atiq M, Bhutani MS, Bektas M, et al. EUS-FNA for pancreatic neuroendocrine tumors: a tertiary cancer center experience. *Dig Dis Sci.* 2012;57:791–800. [PubMed: 21964743]
35. Khashab MA, Yong E, Lennon AM, et al. EUS is still superior to multidetector computerized tomography for detection of pancreatic neuroendocrine tumors. *Gastrointest Endosc.* 2011;73:691–696. [PubMed: 21067742]
36. Jensen RT, Bodei L, Capdevila J, et al. Unmet needs in functional and nonfunctional pancreatic neuroendocrine neoplasms. *Neuroendocrinology.* 2019;108:26–36. [PubMed: 30282083]
37. Kann PH. Is endoscopic ultrasonography more sensitive than magnetic resonance imaging in detecting and localizing pancreatic neuroendocrine tumors? *Rev Endocr Metab Disord.* 2018;19:133–137. [PubMed: 30267296]
38. Jabło ska B, Gudź A, Hinborch T, et al. Pancreatic cystic tumors: a single-center observational study. *Medicina (Kaunas).* 2023;59:241. [PubMed: 36837443]
39. Zhu JK, Wu D, Xu JW, et al. Cystic pancreatic neuroendocrine tumors: a distinctive subgroup with indolent biological behavior? A systematic review and meta-analysis. *Pancreatol.* 2019;19:738–750. [PubMed: 31160191]
40. Lee NJ, Hruban RH, Fishman EK. Pancreatic neuroendocrine tumor: review of heterogeneous spectrum of CT appearance. *Abdom Radiol (NY).* 2018;43(3025–3034).

41. Kawamoto S, Johnson PT, Shi C, et al. Pancreatic neuroendocrine tumor with cystlike changes: evaluation with MDCT. *AJR Am J Roentgenol.* 2013;200:W283–W290. [PubMed: 23436873]
42. Lee JH, Byun JH, Kim JH, et al. Solid pancreatic tumors with unilocular cyst-like appearance on CT: differentiation from unilocular cystic tumors using CT. *Korean J Radiol.* 2014;15:704–711. [PubMed: 25469081]
43. Manfredi R, Ventriglia A, Mantovani W, et al. Mucinous cystic neoplasms and serous cystadenomas arising in the body-tail of the pancreas: MR imaging characterization. *Eur Radiol.* 2015;25:940–949. [PubMed: 25417125]
44. Roseland ME, Francis IR, Shampain KL, et al. Gastric neuroendocrine neoplasms: a primer for radiologists. *Abdom Radiol (NY).* 2022;47: 3993–4004. [PubMed: 35411433]
45. Corey B, Chen H. Neuroendocrine tumors of the stomach. *Surg Clin North Am.* 2017;97:333–343. [PubMed: 28325190]
46. Varas MJ, Gornals JB, Pons C, et al. Usefulness of endoscopic ultrasonography (EUS) for selecting carcinoid tumors as candidates to endoscopic resection. *Rev Esp Enferm Dig.* 2010;102:577–582. [PubMed: 21039065]
47. Konstantinoff KS, Morani AC, Hope TA, et al. Pancreatic neuroendocrine tumors: tailoring imaging to specific clinical scenarios. *Abdom Radiol (NY).* 2023;48:1843–1853. [PubMed: 36737523]
48. Sato Y, Hashimoto S, Mizuno K-I, et al. Management of gastric and duodenal neuroendocrine tumors. *World J Gastroenterol.* 2016;22: 6817–6828. [PubMed: 27570419]
49. Tsai SD, Kawamoto S, Wolfgang CL, et al. Duodenal neuroendocrine tumors: retrospective evaluation of CT imaging features and pattern of metastatic disease on dual-phase MDCT with pathologic correlation. *Abdom Imaging.* 2015;40:1121–1130. [PubMed: 25504375]
50. Lopez CL, Falconi M, Waldmann J, et al. Partial pancreaticoduodenectomy can provide cure for duodenal gastrinoma associated with multiple endocrine neoplasia type 1. *Ann Surg.* 2013;257:308–314. [PubMed: 22580937]
51. McLean AM, Fairclough PD. Endoscopic ultrasound in the localisation of pancreatic islet cell tumours. *Best Pract Res Clin Endocrinol Metab.* 2005; 19:177–193. [PubMed: 15763694]
52. Attili F, Capurso G, Vanella G, et al. Diagnostic and therapeutic role of endoscopy in gastroenteropancreatic neuroendocrine neoplasms. *Dig Liver Dis.* 2014;46:9–17. [PubMed: 23731843]
53. Lee SH, Lee TH, Jang SH, et al. Ampullary neuroendocrine tumor diagnosed by endoscopic papillectomy in previously confirmed ampullary adenoma. *World J Gastroenterol.* 2016;22:3687–3692. [PubMed: 27053861]
54. Li Q-L, Zhang YQ, Chen WF, et al. Endoscopic submucosal dissection for foregut neuroendocrine tumors: an initial study. *World J Gastroenterol.* 2012;18:5799–5806. [PubMed: 23155323]
55. Delle Fave G, O’Toole D, Sundin A, et al. ENETS consensus guidelines update for gastroduodenal neuroendocrine neoplasms. *Neuroendocrinology.* 2016;103:119–124. [PubMed: 26784901]
56. Malla S, Kumar P, Madhusudhan KS. Radiology of the neuroendocrine neoplasms of the gastrointestinal tract: a comprehensive review. *Abdom Radiol (NY).* 2021;46:919–935. [PubMed: 32960304]
57. Boudreaux JP, Klimstra DS, Hassan MM, et al. The NANETS consensus guideline for the diagnosis and management of neuroendocrine tumors: well-differentiated neuroendocrine tumors of the jejunum, ileum, appendix, and cecum. *Pancreas.* 2010;39:753–766. [PubMed: 20664473]
58. Baumann T, Rottenburger C, Nicolas G, et al. Gastroenteropancreatic neuroendocrine tumours (GEP-NET) - imaging and staging. *Best Pract Res Clin Endocrinol Metab.* 2016;30:45–57. [PubMed: 26971843]
59. Olpin J, Fine GC, Shaaban A. Imaging of gastrointestinal neuroendocrine tumors. *Curr Radiol Rep.* 2020;8.
60. Johanssen S, Boivin M, Lochs H, et al. The yield of wireless capsule endoscopy in the detection of neuroendocrine tumors in comparison with CT enteroclysis. *Gastrointest Endosc.* 2006;63:660–665. [PubMed: 16564869]

61. Pilleul F, Penigaud M, Milot L, et al. Possible small-bowel neoplasms: contrast-enhanced and water-enhanced multidetector CT enteroclysis. *Radiology*. 2006;241:796–801. [PubMed: 17053201]
62. Danti G, Flammia F, Matteuzzi B, et al. Gastrointestinal neuroendocrine neoplasms (GI-NENs): hot topics in morphological, functional, and prognostic imaging. *Radiol Med*. 2021;126:1497–1507. [PubMed: 34427861]
63. Kobayashi K, Katsumata T, Yoshizawa S, et al. Indications of endoscopic polypectomy for rectal carcinoid tumors and clinical usefulness of endoscopic ultrasonography. *Dis Colon Rectum*. 2005;48:285–291. [PubMed: 15714250]
64. Walczyk J, Sowa-Staszczak A. Diagnostic imaging of gastrointestinal neuroendocrine neoplasms with a focus on ultrasound. *J Ultrason*. 2019; 19:228–235. [PubMed: 31807329]
65. Caplin M, Sundin A, Nillson O, et al. ENETS consensus guidelines for the management of patients with digestive neuroendocrine neoplasms: colorectal neuroendocrine neoplasms. *Neuroendocrinology*. 2012;95: 88–97. [PubMed: 22261972]
66. Shah R, Nalamati SPM. Neuroendocrine tumors of the colon and rectum. *Semin Colon Rectal Surg*. 2015;26:60–63.
67. Caplin ME, Baudin E, Ferolla P, et al. Pulmonary neuroendocrine (carcinoid) tumors: European Neuroendocrine Tumor Society expert consensus and recommendations for best practice for typical and atypical pulmonary carcinoids. *Ann Oncol*. 2015;26:1604–1620. [PubMed: 25646366]
68. Walker CM, Vummidi D, Benditt JO, et al. What is DIPNECH? *Clin Imaging*. 2012;36:647–649. [PubMed: 22920384]
69. Chassagnon G, Favelle O, Marchand-Adam S, et al. DIPNECH: when to suggest this diagnosis on CT. *Clin Radiol*. 2015;70:317–325. [PubMed: 25465294]
70. Foran PJ, Hayes SA, Blair DJ, et al. Imaging appearances of diffuse idiopathic pulmonary neuroendocrine cell hyperplasia. *Clin Imaging*. 2015;39:243–246. [PubMed: 25496668]
71. Ruffini E, Bongiovanni M, Cavallo A, et al. The significance of associated pre-invasive lesions in patients resected for primary lung neoplasms. *Eur J Cardiothorac Surg*. 2004;26:165–172. [PubMed: 15200997]
72. Gustafsson BI, Kidd M, Chan A, et al. Bronchopulmonary neuroendocrine tumors. *Cancer*. 2008;113:5–21. [PubMed: 18473355]
73. Chong S, Lee KS, Chung MJ, et al. Neuroendocrine tumors of the lung: clinical, pathologic, and imaging findings. *Radiographics*. 2006;26: 41–57 discussion 57–8. [PubMed: 16418242]
74. Ramirez RA, Chauhan A, Gimenez J, et al. Management of pulmonary neuroendocrine tumors. *Rev Endocr Metab Disord*. 2017;18:433–442. [PubMed: 28868578]
75. Meisinger QC, Klein JS, Butnor KJ, et al. CT features of peripheral pulmonary carcinoid tumors. *AJR Am J Roentgenol*. 2011;197: 1073–1080. [PubMed: 22021498]
76. Gridelli C, Rossi A, Airoma G, et al. Treatment of pulmonary neuroendocrine tumours: state of the art and future developments. *Cancer Treat Rev*. 2013;39:466–472. [PubMed: 22818212]
77. Kim HS, Lee KS, Ohno Y, et al. PET/CT versus MRI for diagnosis, staging, and follow-up of lung cancer. *J Magn Reson Imaging*. 2015;42: 247–260. [PubMed: 25365936]
78. Sorbye H, Grande E, Pavel M, et al. European Neuroendocrine Tumor Society (ENETS) 2023 guidance paper for digestive neuroendocrine carcinoma. *J Neuroendocrinol*. 2023;35:e13249. [PubMed: 36924180]
79. Pavel M, O’Toole D, Costa F, et al. ENETS consensus guidelines update for the management of distant metastatic disease of intestinal, pancreatic, bronchial neuroendocrine neoplasms (NEN) and NEN of unknown primary site. *Neuroendocrinology*. 2016;103:172–185. [PubMed: 26731013]
80. Kirshbom PM, Kherani AR, Onaitis MW, et al. Carcinoids of unknown origin: comparative analysis with foregut, midgut, and hindgut carcinoids. *Surgery*. 1998;124:1063–1070. [PubMed: 9854584]
81. Sampathirao N, Basu S. MIB-1 index-stratified assessment of dual-tracer PET/CT with 68Ga-DOTATATE and 18F-FDG and multimodality anatomic imaging in metastatic neuroendocrine tumors of unknown primary in a PRRT workup setting. *J Nucl Med Technol*. 2017;45:34–41. [PubMed: 28154019]

82. Riihimäki M, Hemminki A, Sundquist K, et al. The epidemiology of metastases in neuroendocrine tumors. *Int J Cancer*. 2016;139:2679–2686. [PubMed: 27553864]
83. Park HK, Kwon GY. Comparison of metastatic patterns among neuroendocrine tumors, neuroendocrine carcinomas, and nonneuroendocrine carcinomas of various primary organs. *J Korean Med Sci*. 2023;38:e85. [PubMed: 36942393]
84. Joseph S, Wang YZ, Boudreaux JP, et al. Neuroendocrine tumors: current recommendations for diagnosis and surgical management. *Endocrinol Metab Clin N Am*. 2011;40:205–231.
85. Lestra T, Kanagaratnam L, Mulé S, et al. Measurement variability of liver metastases from neuroendocrine tumors on different magnetic resonance imaging sequences. *Diagn Interv Imaging*. 2018;99:73–81. [PubMed: 29339222]
86. Baxi AJ, Chintapalli K, Katkar A, et al. Multimodality imaging findings in carcinoid tumors: a head-to-toe Spectrum. *Radiographics*. 2017;37: 516–536. [PubMed: 28287937]
87. d'Assignies G, Fina P, Bruno O, et al. High sensitivity of diffusion-weighted MR imaging for the detection of liver metastases from neuroendocrine tumors: comparison with T2-weighted and dynamic gadolinium-enhanced MR imaging. *Radiology*. 2013;268:390–399. [PubMed: 23533288]
88. Tirumani SH, Jagannathan JP, Braschi-Amirfarzan M, et al. Value of hepatocellular phase imaging after intravenous gadoxetate disodium for assessing hepatic metastases from gastroenteropancreatic neuroendocrine tumors: comparison with other MRI pulse sequences and with extracellular agent. *Abdom Radiol (NY)*. 2018;43:2329–2339. [PubMed: 29470627]
89. Tsutsumi K, Ohtsuka T, Mori Y, et al. Analysis of lymph node metastasis in pancreatic neuroendocrine tumors (PNETs) based on the tumor size and hormonal production. *J Gastroenterol*. 2012;47:678–685. [PubMed: 22350698]
90. Zaidi MY, Lopez-Aguilar AG, Dillhoff M, et al. Prognostic role of lymph node positivity and number of lymph nodes needed for accurately staging small-bowel neuroendocrine tumors. *JAMA Surg*. 2019;154: 134–140. [PubMed: 30383112]
91. Starzy ska T, Londzin-Olesik M, Bałdys-Waligórska A, et al. Colorectal neuroendocrine neoplasms - management guidelines (recommended by the Polish Network of Neuroendocrine Tumours). *Endokrynol Pol*. 2017; 68:250–260. [PubMed: 28540975]
92. Pirasteh A, Lovrec P, Bodei L. Imaging of neuroendocrine tumors: a pictorial review of the clinical value of different imaging modalities. *Rev Endocr Metab Disord*. 2021;22:539–552. [PubMed: 33783695]
93. Prasad V, Ambrosini V, Hommann M. Detection of unknown primary neuroendocrine tumours (CUP-NET) using (68)Ga-DOTA-NOC receptor PET/CT. *Eur J Nucl Med Mol Imaging*. 2010;37:67–77. [PubMed: 19618183]
94. Schraml C, Schwenzer NF, Sperling O, et al. Staging of neuroendocrine tumours: comparison of [⁶⁸Ga]DOTATOC multiphase PET/CT and whole-body MRI. *Cancer Imaging*. 2013;13:63–72. [PubMed: 23466785]
95. Putzer D, Gabriel M, Henninger B, et al. Bone metastases in patients with neuroendocrine tumor: 68Ga-DOTA-Tyr3-octreotide PET in comparison to CT and bone scintigraphy. *J Nucl Med*. 2009;50:1214–1221. [PubMed: 19617343]
96. Altieri B, Di Dato C, Martini C, et al. Bone metastases in neuroendocrine neoplasms: from pathogenesis to clinical management. *Cancers (Basel)*. 2019;11:1332. [PubMed: 31500357]
97. Meijer WG, van der Veer E, Jager PL, et al. Bone metastases in carcinoid tumors: clinical features, imaging characteristics, and markers of bone metabolism. *J Nucl Med*. 2003;44:184–191. [PubMed: 12571207]
98. O'Sullivan GJ, Carty FL, Cronin CG. Imaging of bone metastasis: an update. *World J Radiol*. 2015;7:202–211. [PubMed: 26339464]
99. Martin S, Iravani A, Shetty AS, et al. Neuroendocrine neoplasm imaging: protocols by site of origin. *Abdom Radiol (NY)*. 2022;47(4081–4095).
100. Kos-Kudła B, O'Toole D, Falconi M, et al. ENETS consensus guidelines for the management of bone and lung metastases from neuroendocrine tumors. *Neuroendocrinology*. 2010;91:341–350. [PubMed: 20484875]



FIGURE 1.

Axial non-CE T1w fat-saturated (A), arterial phase T1w fat-saturated (B), and T2w SSFSE fat-saturated images. On non-CE T1w fat-saturated images (A), NETs (arrow) tend to be hypointense, compared to a healthy pancreas. In arterial phase imaging (B), they usually enhance more avidly than normal background parenchyma. They also present hyperintense on T2w imaging (C).

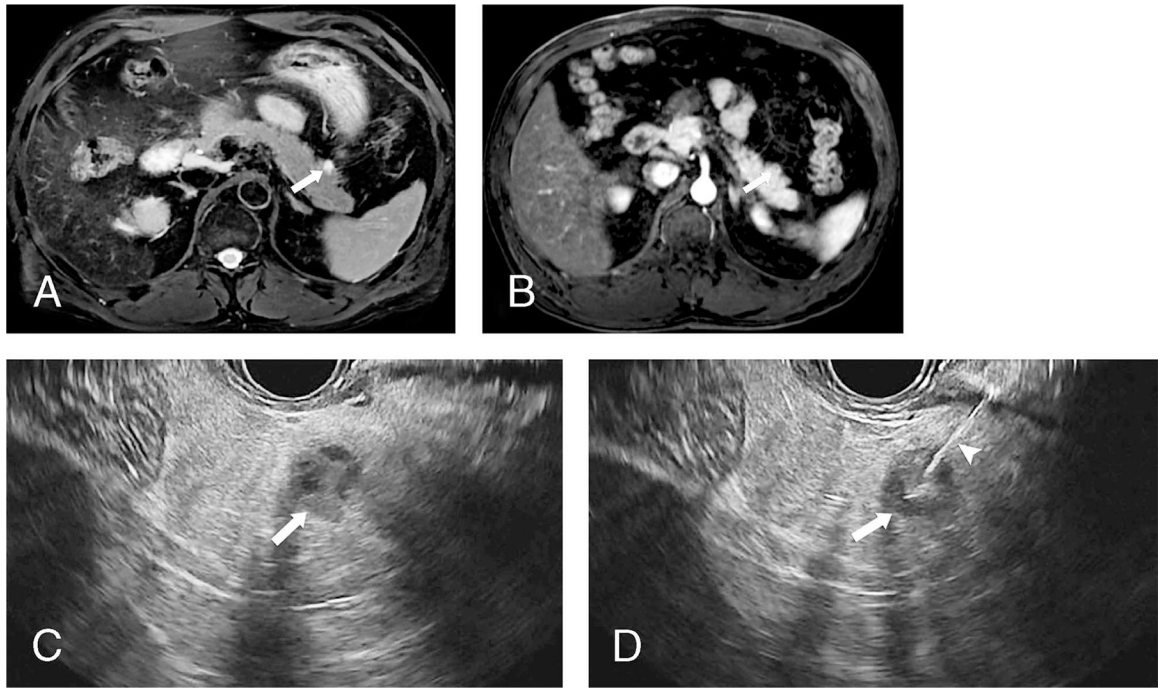
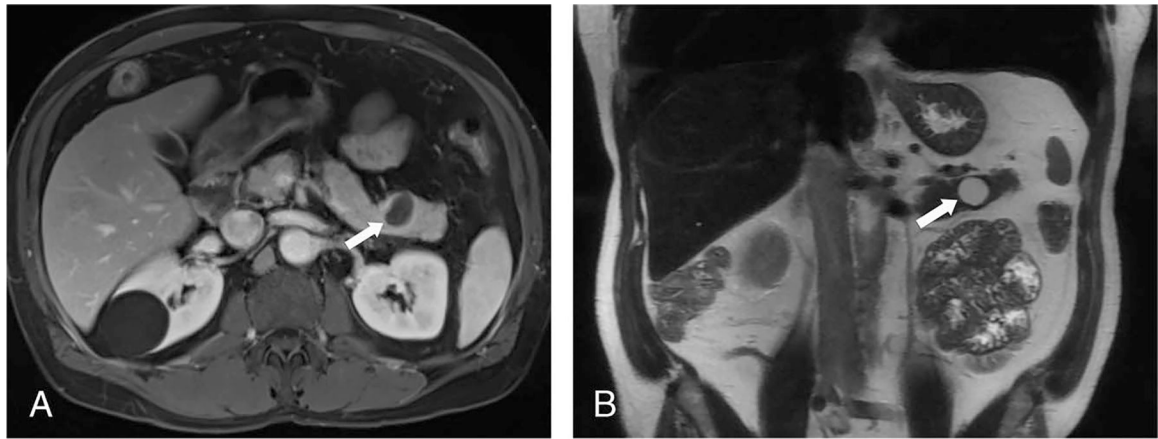


FIGURE 2.

Axial T2w fat-saturated SSFSE (A), T1w arterial phase (B), and EUS (C and D) images. A 6-mm pancreatic tail grade 2 NET (arrow), given its high T2w signal intensity (A), is easily detected; lesion enhancement (B) rules out cystic entities. EUS, due to its superior resolution, better visualizes the NET, which presents as a well-circumscribed hypoechoic lesion (C) and also allows for definitive diagnosis through tissue sampling (arrowhead) (D).

**FIGURE 3.**

Axial T1w portal venous phase (A) and coronal T2w SSFSE (B) images. A cystic lesion (arrow) in the pancreatic tail demonstrates a thick, smooth, and uniform rind of peripheral enhancement (A). There are no internal septa nor communication with the pancreatic duct (B). These features favor a cystic pancreatic NET, as subsequently confirmed by tissue sampling.

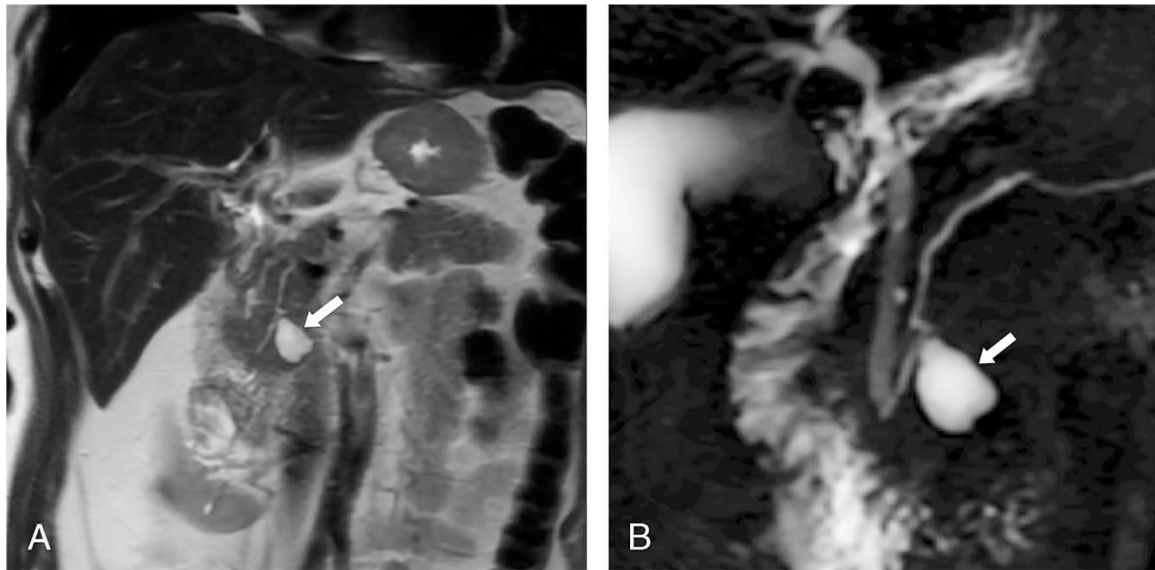


FIGURE 4. Coronal T2w SSFSE (A) and MRCP (B) images. Cystic lesion in the pancreatic head communicates with the pancreatic duct (arrow). Duct communication excludes a cystic NET and is diagnostic of the pancreas's side branch intraductal papillary mucinous neoplasm.

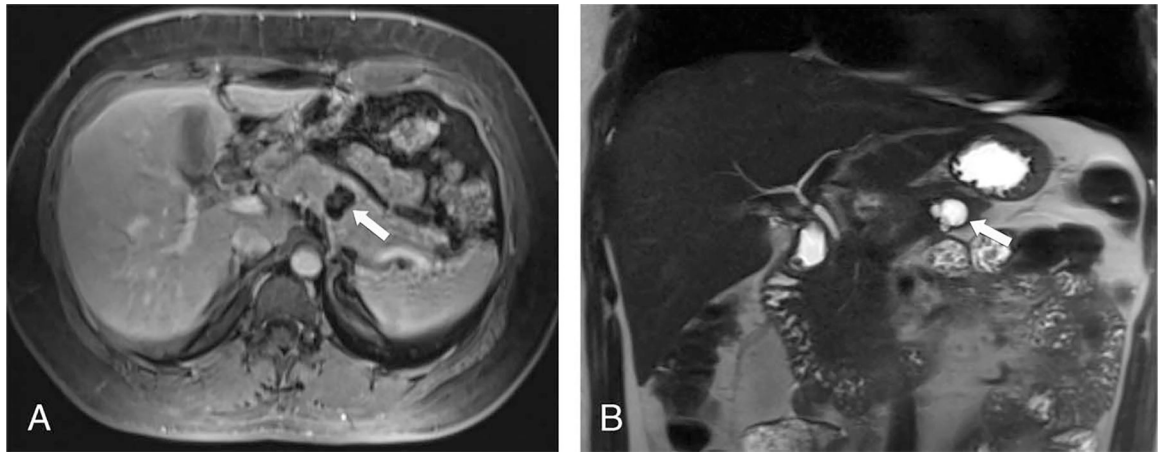


FIGURE 5.

Axial T1w portal venous phase (A) and coronal T2w SSFSE (B) images. A cystic lesion (arrow) in the pancreatic body demonstrates a thick rind of peripheral enhancement and does not communicate with the pancreatic duct. However, this cystic lesion presents a lobulated contour and contains enhancing internal septa; these features are more in favor of other etiologies, including mucinous cystic neoplasm, as subsequently pathologically confirmed, rather than of NETs.

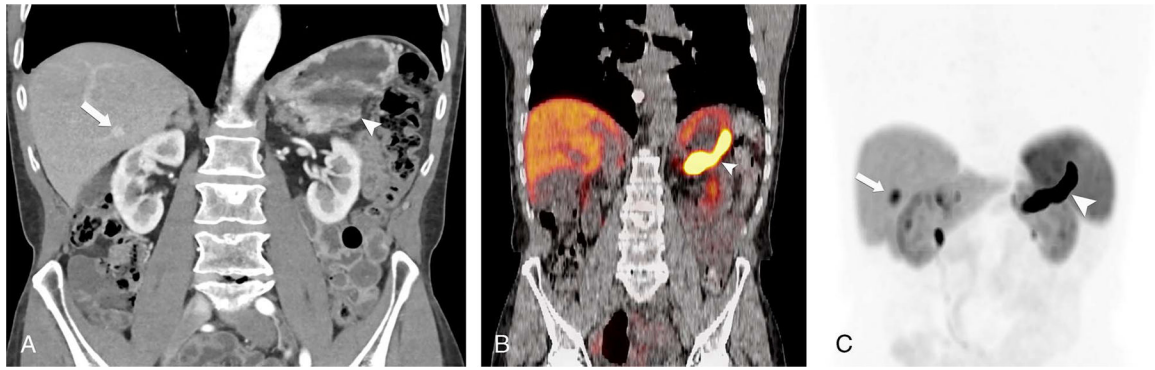


FIGURE 6.

Coronal arterial phase CE-CT (A), fused DOTATE PET/CT (B), and coronal DOTATATE PET (C). Primary cystic pancreatic NET (arrowhead) demonstrates marked DOTATATE uptake in its walls. A focal hepatic lesion (arrow) displays marked arterial enhancement and radiotracer avidity, as per NET metastasis.

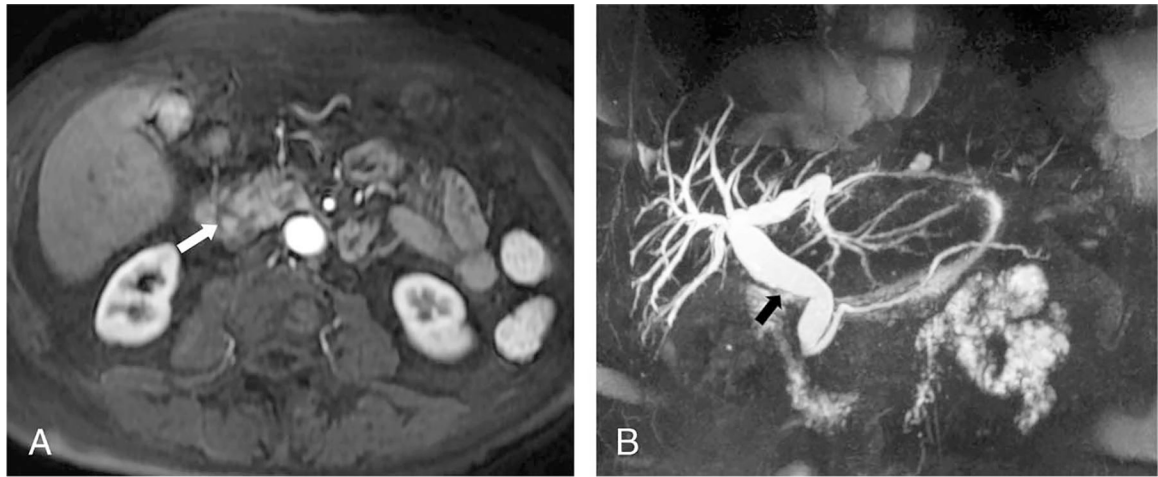
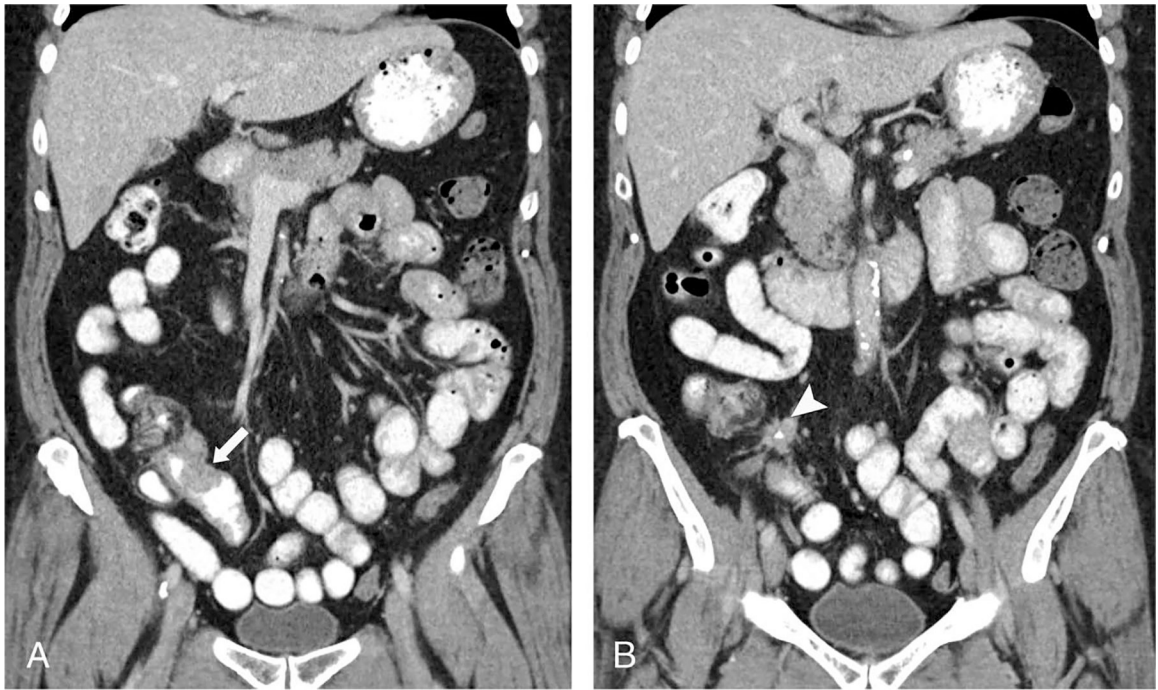


FIGURE 7. Axial T1w arterial phase (A) and coronal MRCP (B) images. Despite even severe biliary duct dilation (black arrow), diagnosis of ampullary NETs (arrow) might be challenging, especially if of small size. However, arterial phase imaging can facilitate detection.

**FIGURE 8.**

Coronal CE-CT (A and B). Small bowel NETs (arrow) tend to occur in the last 100 cm of the distal ileum and present as focal wall thickening. Bowel distention with oral contrast facilitates detection. Associated mesenteric lymphadenopathy and desmoplastic reaction (arrowhead) tend to occur close to the primary tumor, can harbor calcifications, and can tether bowel loops.

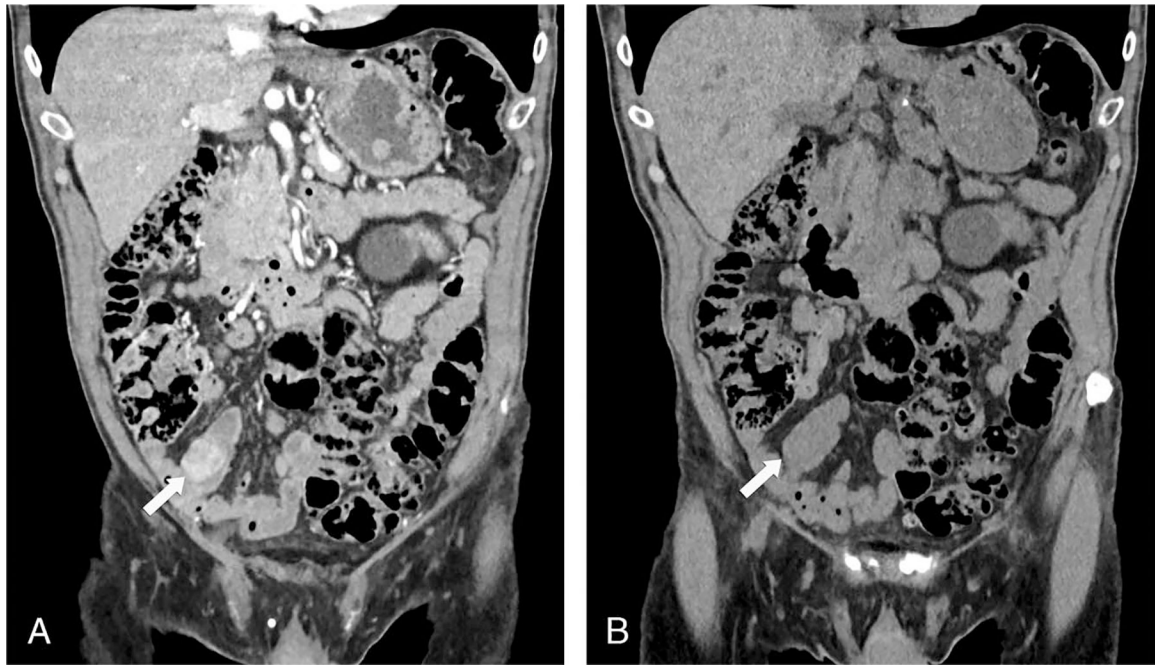


FIGURE 9.

CT-enterography with (A) and without (B) intravenous contrast. Distal ileum is distended by fluid and contains a large and markedly enhancing polypoid NEN (arrow). The lesion, which immediately stands out after contrast injection, would be extremely hard to diagnose on non-CE CT image (B). Usage of oral and intravenous contrast facilitates detection of SB-NENs.



FIGURE 10.

Coronal T1w fat-saturated (A), T2w SSFSE fat-saturated (B), and T1w fat-saturated CE (C) images. In MRI, similarly to CT, usage of oral and intravenous contrast helps detection of NENs (arrows). These tumors would be very challenging to appreciate in the case of collapsed bowel loops and absence of intravenous contrast.

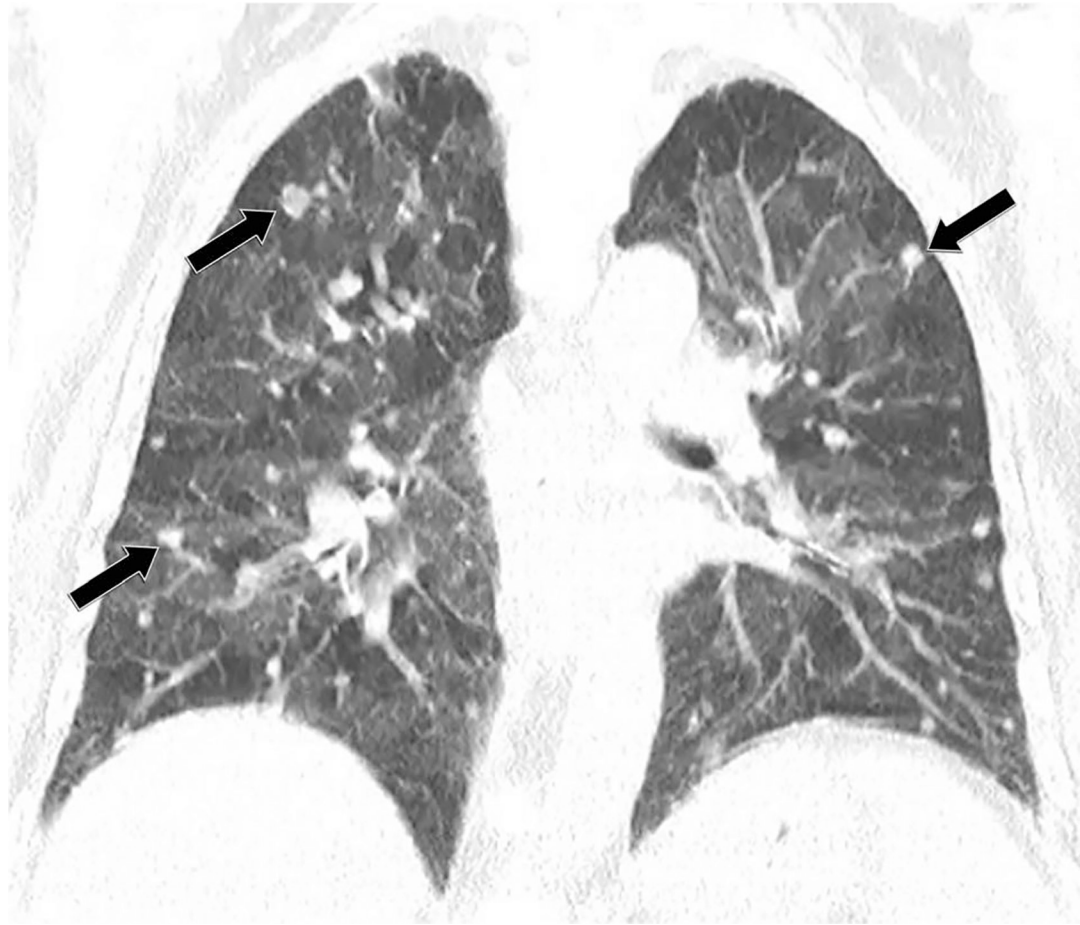


FIGURE 11. Coronal CT image. Multiple bilateral pulmonary nodules (arrows) and mosaic attenuation. Wedge resection of the left upper and lower lobes demonstrates carcinoid tumors and tumorlets, and neuroendocrine cell hyperplasia within airway epithelium in keeping with DIPNECH.

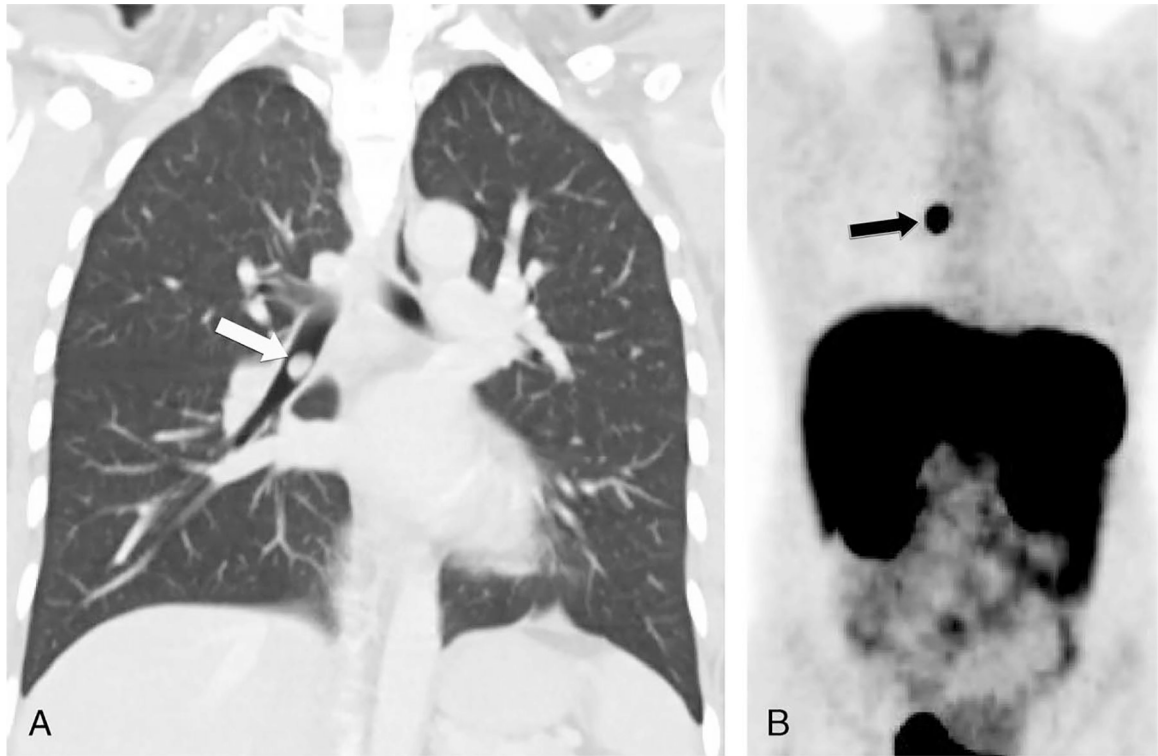


FIGURE 12. Axial CT (A) and DOTATATE PET (B) images. There is an endobronchial nodule in the bronchus intermedius (arrow), which demonstrates marked DOTATATE PET uptake (arrow). This was confirmed to be a typical carcinoid on resection.

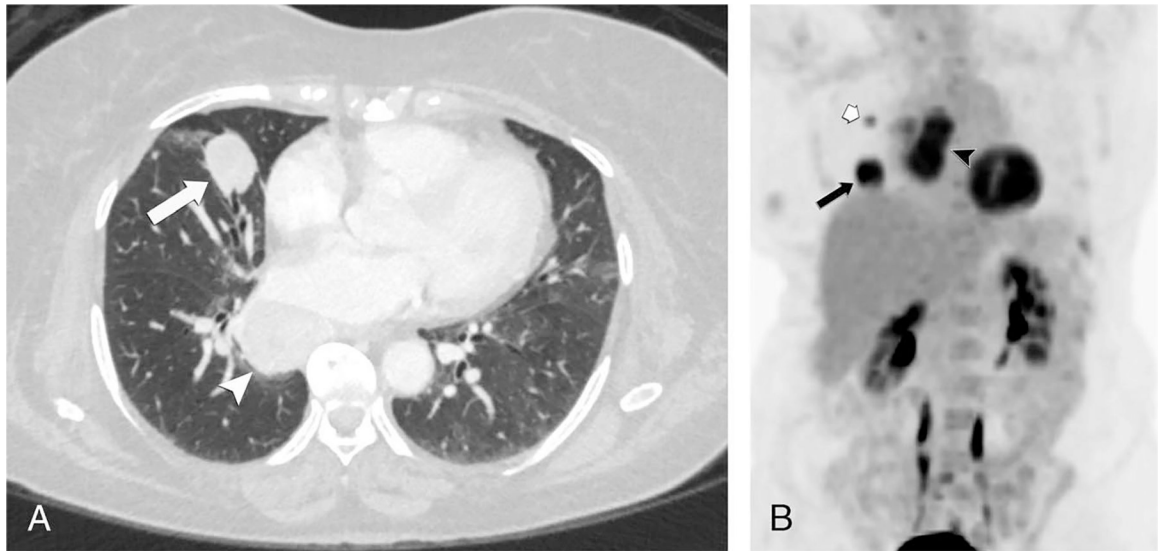


FIGURE 13.

Axial CT (A) and FDG PET (B) were imaged. There is a dominant nodule in the right middle lobe (arrow) and subcarinal adenopathy (arrowhead), which, along with another right lung nodule (white short arrow), demonstrates marked FDG activity. This was confirmed to be an atypical carcinoid on biopsy.



FIGURE 14. Monochromatic (A) and nonmonochromatic (B) CE-CT images. Monochromatic images increase the conspicuity of contrast enhancement among anatomic structures and tissues, facilitating the detection of hypervascular NEN metastases (arrows) to the liver, which could have otherwise blended with similar attenuation background hepatic parenchyma as in B.



FIGURE 15. Sagittal CT (A) and STIR (B) images. NEN metastases to the bones (arrow) tend to present sclerotic as in A. MRI outperforms CT in detecting additional early metastases (arrowhead), which otherwise could be completely undetected on CT.

TABLE 1.

Imaging protocols for Neuroendocrine Neoplasms

Imaging Protocol	Phases/Sequences	Contrast Agents	Additional Considerations
Pancreatic protocol CT	Noncontrast, late arterial, portal venous	Iodinated intravenous contrast	Optional 120-s delayed phase for neuroendocrine tumors Negative oral contrast for gastric/distal lesion visibility. Avoid positive oral contrast
Liver protocol CT	Late arterial, portal venous, delayed	Iodinated intravenous contrast	Noncontrast phase for cases with prior liver therapy. Consider MR in cases with lipiodol therapy
CT enterography (CTE)	Multiphase with negative oral contrast	Iodinated intravenous contrast	Fasting 4–6 h before imaging, consider SSTR PET/CT
Pancreatic protocol MRI	T2WI, chemical shift imaging, DWI, contrast	Extracellular contrast agents	Consider MRCP for ductal involvement, avoid positive oral contrast
Liver protocol MRI	Dynamic phases, T2WI, 2D/3D MRCP	Extracellular or hepatobiliary contrast	Include entire liver in FOV, consider hepatobiliary contrast for liver-directed treatment
MR enterography (MRE)	T1WI, T2WI, dynamic postcontrast	Biphasic contrast (VoLumen)	Fasting 4–6 h before imaging, consider glucagon to reduce bowel peristalsis
PET/CT (SSTR-PET/CT)	CT (noncontrast/portal venous/multiphase)	PET (somatostatin or FDG)	Avoid barium, good hydration, consider patient's treatment timing
PET/MRI	Same as PET/CT	Same as PET/CT	Limited availability, may offer advantages.